Bioorganic & Medicinal Chemistry 20 (2012) 4330–4335

Contents lists available at SciVerse ScienceDirect

Bioorganic & Medicinal Chemistry

journal homepage: www.elsevier.com/locate/bmc

Synthesis and evaluation of a radioiodinated bladder cancer specific peptide

Yeong Su Ha [a,†], Hwa Young Lee [a,†], Gwang Il An [b], Jonghee Kim [a], Wonjung Kwak [a], Eun-Ju Lee [c], Seung-Min Lee [c], Byung-Heon Lee [c], In-San Kim [c], Takele Belay [a], Woonghee Lee [a], Byeong-Cheol Ahn [d], Jaetae Lee [d], Jeongsoo Yoo [a,*]

[a] Department of Molecular Medicine, Kyungpook National University, School of Medicine, Daegu 700-422, South Korea
[b] Molecular Imaging Research Center, Korea Institute of Radiological and Medical Sciences, Seoul, South Korea
[c] Department of Biochemistry and Cell Biology and Cell & Matrix Research Institute, Kyungpook National University, School of Medicine, Daegu, South Korea
[d] Department of Nuclear medicine, Kyungpook National University, School of Medicine, Daegu, South Korea

ARTICLE INFO

Article history:
Received 12 April 2012
Revised 19 May 2012
Accepted 21 May 2012
Available online 29 May 2012

Keywords:
Bladder cancer
Disease-specific peptide
Radiopharmaceuticals
Radioiodination
PET

ABSTRACT

Bladder cancer is the second most common cancer of the urinary tract, however the invasive cystoscopy is still the standard technique for diagnosis and surveillance of bladder cancer. Herein, we radiolabel bladder cancer specific peptide with radioactive iodine ($^{131/124}$I) and evaluate its potential as a new radiopharmaceutical for the non-invasive diagnosis of bladder cancer. A 9-mer bladder cancer specific peptide (BP) was conjugated with tyrosine and cyclized by disulfide bond formation to give Y-BP, which was further radioiodinated to give [$^{131/124}$I]Y-BP in good radiochemical yield. The biodistribution data showed the high selectivity of [^{124}I]Y-BP in HT1376 human bladder cancer xenograft models with a tumor-to-muscle ratio of 6.2. This tumor targeting was not observed in control B16F10 melanoma tumor models. In microPET studies, while the control scrambled peptide, [^{124}I]Y-sBP, did not accumulate in either the bladder cancer or melanoma, [^{124}I]Y-BP showed high tumor uptake only in animals with HT1376 bladder cancer cells. Furthermore, [^{124}I]Y-BP showed superior bladder cancer uptake even compared to most commonly used cancer imaging tracer, [^{18}F]FDG. The experimental results suggest the potential of [^{124}I]Y-BP as a new radiopharmaceutical for the non-invasive diagnosis of bladder cancer with high binding affinity and selectivity.

1. Introduction

Bladder cancer is the second most common cancer of the urinary tract after prostate cancer.[1] About 70% of all bladder cancer patients have superficial cancers. Although superficial cancers can be easily removed by trans-urethral resection, they are associated with a high recurrence rate and 10–20% will progress to muscle invasion.[2] Furthermore, following radical cystectomy, up to 50% of patients will develop metastases.[3] Because of its high recurrence rate, which is the highest of all cancers, surveillance of bladder cancer patients needs to be very rigorous.

Cystoscopy and urine cytology are the traditional techniques for diagnosis and surveillance of bladder cancer. Cystoscopy is invasive and lacks specificity for flat malignancies[4–6], though it can visualize the urothelium of the bladder wall directly. And, the use of cystoscopy is restricted to primary cancer inside bladder, but the metastasized tumor to other organs cannot be diagnosed by this technique. Cytology is a convenient non-invasive test for patients with history of bladder cancer and for screening of high-risk populations. However, clinical experience has shown limitations of urine cytology in low grade cancers, in which the sensitivity is low.[7,8] Several urine markers have shown higher sensitivity than urine cytology, however most of these markers tend to be less specific for bladder cancer than cytology.[6] These characteristics of current diagnosis techniques have prompted the search for more reliable non-invasive imaging methods for bladder cancer.

Positron emission tomography (PET) using fluorine-18 fluoro-2-deoxy-D-glucose ([^{18}F]FDG) has been shown to be an accurate technique for cancer detection and staging and for the monitoring of therapy in patients with various malignant cancers.[9,10] Because [^{18}F]FDG is an analog of glucose, it is taken up by the cells via the glucose transporter and are then phosphorylated by the hexokinase, but the product, fluoro-2-deoxyglucose-6-phosphate is not further processed and trapped in the cells. Hence, the accumulation of [^{18}F]FDG is an indicator of high glucose uptake rate and hexokinase activity in the tissue. However, clinical experience with FDG–PET in bladder cancer has revealed a major disadvantage of FDG: the excretion of radioactivity into urine, causing accumulation of activity in the bladder.[11,12] Furthermore, because of relatively short half-life of F-18 (110 min), the late imaging, in which most activity is cleared out from non-specific organs, is not feasible. Another disadvantage of FDG–PET imaging is an inherent

* Corresponding author. Tel.: +82 53 420 4947; fax: +82 53 426 4944.
E-mail address: yooj@knu.ac.kr (J. Yoo).
† These authors contributed equally.

0968-0896/$ - see front matter © 2012 Elsevier Ltd. All rights reserved.
http://dx.doi.org/10.1016/j.bmc.2012.05.049

background signal.[13] Basically, all cells metabolize glucose and some glucose-avid organs such as brain, heart and brown fat always show intense FDG background signal.

In the past decade, new radiopharmaceuticals based on small synthetic peptides have been developed for tumor imaging and targeted radiotherapy.[14–20] Radiopharmaceuticals based on peptides have a number of distinct advantages over those based on proteins or antibodies, including their small size, easy preparation, site-specific radiolabeling, toleration of harsh conditions of conjugation or radiolabeling, rapid clearance from blood and non-target tissues, high penetration into tumor tissue, and low immunogenicity.[14,16]

Recently, Lee et al. identified a small peptide which shows high binding affinity for bladder cancer using phage-displayed peptide libraries.[21] The fluorescein-conjugated CSNRDARRC peptide was found to bind selectively to bladder cancer tissue and it also selectively labeled cancer cells in urine of patients with bladder cancer.

Here, we radiolabel this bladder cancer specific peptide with PET radionuclide, ^{124}I, and evaluate its potential as a new radiopharmaceutical for the diagnosis of bladder cancer in in vivo tumor models.

2. Results and discussion

2.1. Peptide preparation and radiochemistry

The bladder cancer specific peptide, which was found by phage display screening,[21,22] was first conjugated to tyrosine residue for radioiodination and cyclized using the two cysteine residues at the terminal positions to inhibit the in vivo proteolysis of the peptides.[16] Both bladder cancer specific peptide, Y-BP, and its scrambled version, Y-*s*BP were prepared in >98% chemical purities, purified by HPLC, and characterized by mass analysis (Fig. 1). Experimental MS (ESI) data were well matched with the expected values (calculated for Y-BP: 1240.52, found: 1241; calculated for Y-*s*BP: 1240.52, found: 1240).

These two peptides were then radiolabeled with ^{131}I or ^{124}I using tyrosine group on *N*-terminal (Fig. 2). Among the various radiolabeling methods, radioiodination was chosen, because various iodine radionuclides such as ^{123}I, ^{124}I, ^{125}I, ^{131}I are available and radiolabeling can be achieved easily by direct iodination via the phenolic ring of the tyrosine residue in the presence of an oxidizing agent such as Iodo-beads and Iodogen.[15,23] We used a positron-emitting ^{124}I (23% of disintegration, $t_{1/2}$ 4.2 d) for microPET imaging,[24] but in pre-imaging studies, γ-ray emitting ^{131}I was employed as radioactive iodine source because high purity ^{131}I is easily available while ^{124}I is produced in limited quantity only for research purpose yet. The another beauty of ^{131}I is its long half-life (8.0 d) and the following experiments can be performed without restriction from decay loss.

The radiolabeling yield of Y-BP with ^{131}I and ^{124}I was >30% and >23%, respectively, using Iodo-beads. However, when the labeling method was changed to Iodogen (Pierce) from Iodo-beads, the radiolabeling yield with ^{131}I and ^{124}I dramatically increased to >90% and >60%, respectively. The radiolabeling yield was always higher when using I-131 compared to I-124, presumably due to higher specific activity of I-131 over I-124. The radiolabeling yields of Y-*s*BP was comparable with those of Y-BP. The labeled peptides were purified by reverse-phase HPLC to give [$^{131/124}$I]Y-BP and [^{124}I]Y-*s*BP in >98% radiochemical purities (Fig. 3). The purified radioiodinated peptides were used for following in vitro and in vivo studies.

Peptide	Sequence
Y-BP	Tyr-Cys-Ser-Asn-Arg-Asp-Ala-Arg-Arg-Cys (S—S)
Y-*s*BP	Tyr-Cys-Asp-Ala-Ser-Arg-Arg-Asn-Arg-Cys (S—S)

Figure 1. Peptide sequences of bladder cancer specific peptide (Y-BP) and control peptide having scrambled sequence (Y-*s*BP).

2.2. Serum stability test

To ensure that the radiolabeled peptide remains intact in vivo long enough to target the bladder cancer specific receptors, we studied the stability of radioiodinated bladder cancer specific peptide in serum. The HPLC purified [^{131}I]Y-BP was incubated with FBS and PBS at 37 °C for up to 24 h. The relative amount of intact parent radiolabled peptide was determined using radio-TLC over the study period. The results of radio-TLC analyses indicated that more than 60% of intact peptide remained after a 5 h incubation in FBS, which could be fairly enough for microPET imaging (Fig. 4). After 24 h in FBS, only 37% of intact peptide remained, which is far lower than 88% in PBS.

2.3. MicroPET imaging

The specific binding of the radiolabeled [^{124}I]Y-BP to the bladder cancer was evaluated by microPET imaging studies using xenograft tumor models.

The typical images of the comparative microPET imaging studies of [^{124}I]Y-BP and [^{124}I]Y-*s*BP in the nude mice bearing HT1376 bladder cancer and B16F10 melanoma cells on each flank side are shown in Figure 6. While the bladder cancer HT1376 was clearly visualized, the uptake level of [^{124}I]Y-BP in melanoma B16F10 is as low as the background at 5.5 h post-injection. The uptake activity in HT1376 bladder cancer model (1.2%ID/g in tumor) was 4.6 fold higher than that of B16F10 melanoma tumor model. At earlier time points (30 min, 2 h), the tumor-to-background ratio was insufficiently high (1.7 and 2.0, respectively) for the tumor region to be clearly visualized. Thanks to enough long half-life of ^{124}I (4.2 d), up to one day image could be measured without difficulty even though tumor-to-background ratio was slowly decreased after 5.5 h (5.4 and 1.9 at 5.5 and 15 h, respectively). In addition, the control peptide [^{124}I]Y-*s*BP did not show any noticeable tumor uptake both in HT1376 bladder tumor (0.4%ID/g) and B16F10 melanoma xenografts. This microPET data is well consistent with the previous in vivo targeting studies of the fluorescein-conjugated CSNRDARRC peptide.[23] In both microPET studies, the thyroid and stomach showed very intense activity uptake due to the free ^{124}I ions released from the injected peptides under physiological conditions. This is not unexpected, as de-iodination in vivo of directly radioiodinated peptide has already been reported as an inevitable phenomenon.[25] This de-iodination in physiological condition was also expected from the in vitro serum stability test of [^{131}I]Y-BP.

The potential of [^{124}I]Y-BP to be used as a radiotracer for the diagnosis of bladder cancer was further examined by direct microPET comparison studies with the most widely employed tumor imaging tracer, [^{18}F]FDG in the same tumor model.[13] In this experiment, the free radioactive iodine uptake in thyroid and stomach was minimized by pre-injection of sodium perchlorate ($NaClO_4$) before [^{124}I]Y-BP injection.[26]

The tumor lesion in HT1376 bladder cancer bearing xenografts was recognized using both [^{124}I]Y-BP and [^{18}F]FDG as a PET radiotracers at 5.5 h and 40 min post-injection, respectively (Fig. 7). However, while HT1376 cancer was barely recognized by

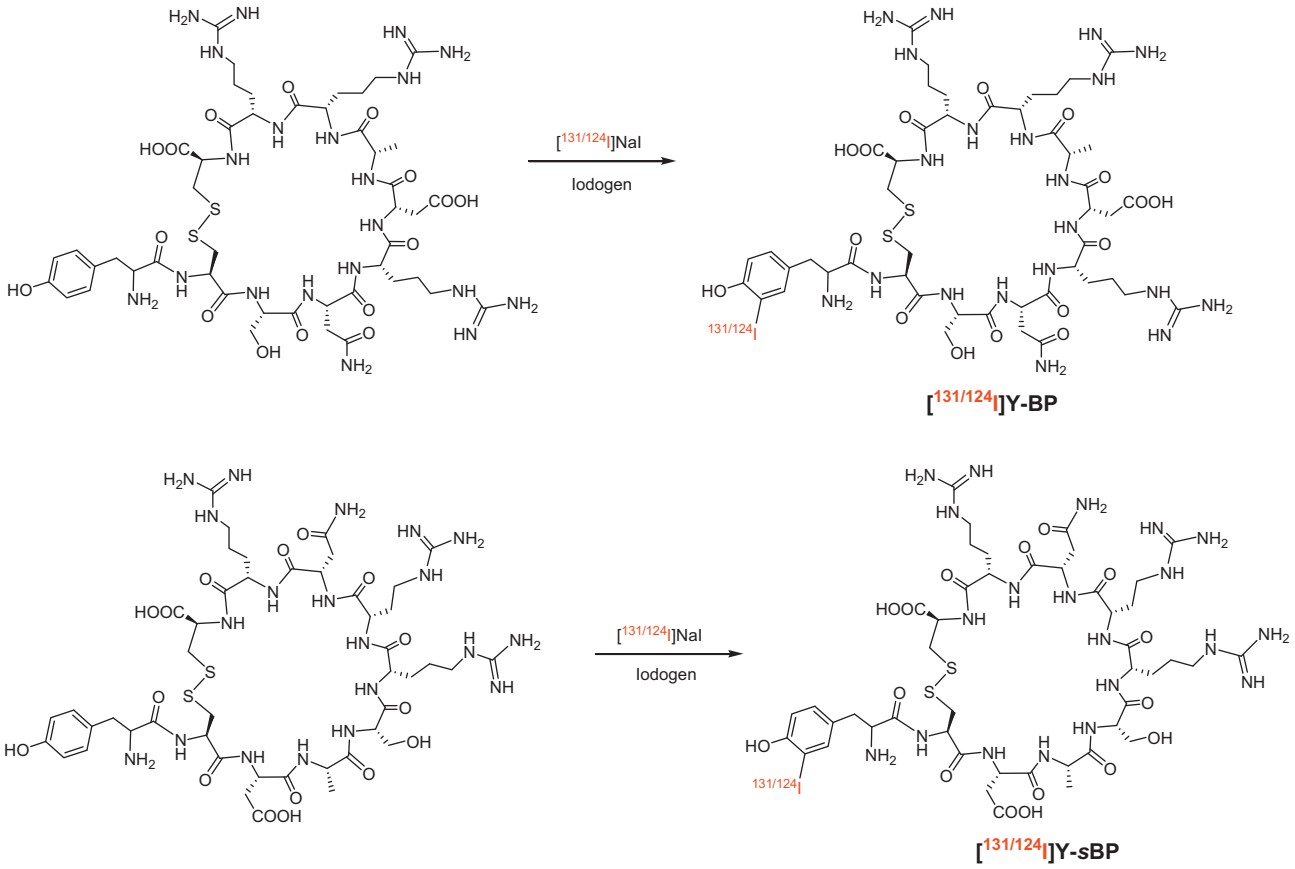

Figure 2. Chemical structures of radiolabeled [$^{131/124}$I]Y-BP and [$^{131/124}$I]Y-*s*BP.

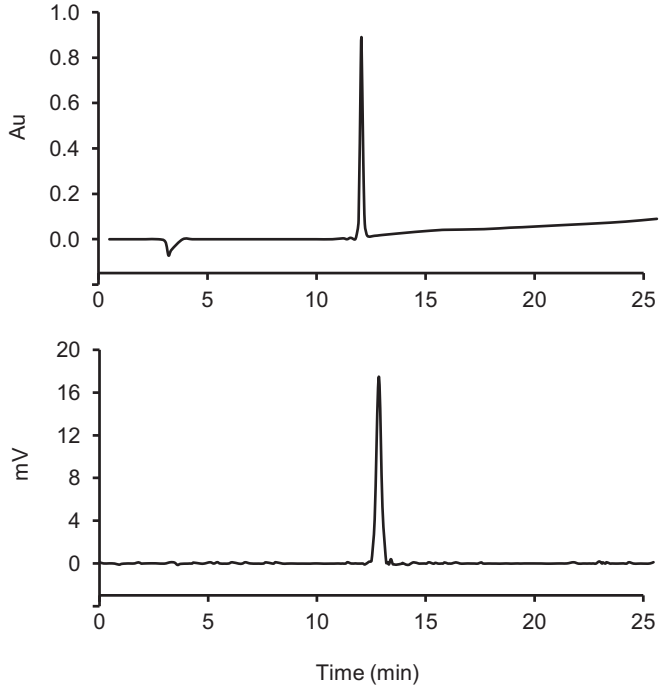

Figure 3. UV chromatogram of non-radiolabeled Y-BP at 220 nm wavelength (top) and radio tracer of [^{124}I]Y-BP after HPLC purification (bottom).

[^{18}F]FDG, the same tumor was unambiguously visualized using [^{124}I]Y-BP. There is little background in microPET image of [^{124}I]Y-BP except hot bladder. The tumor-to-background ratio of

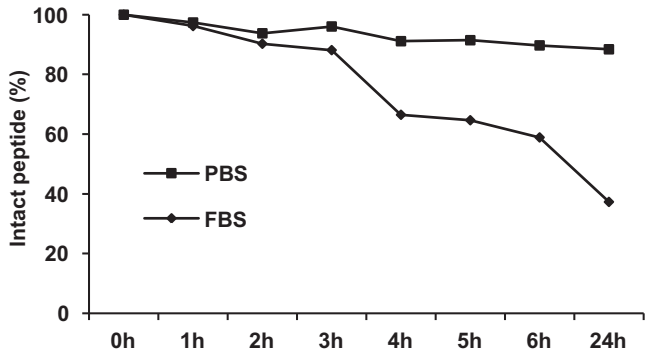

Figure 4. Serum stability of [^{131}I]Y-BP in PBS and FBS.

[^{124}I]Y-BP and [^{18}F]FDG was calculated to be 5.4 and 2.5, respectively, which clearly says that [^{124}I]Y-BP is superior to [^{18}F]FDG in visualizing bladder cancer. Thanks to the blocking of free ^{124}I in thyroid and stomach using sodium perchlorate, the background level in [^{124}I]Y-BP image was lower compared to the previous images in Fig. 6. However, the clearance organ, bladder showed much higher radioactivity. In [^{18}F]FDG image, high glucose-consuming lesions such as brain and brown fat showed higher uptake of [^{18}F]FDG than tumor.[27]

2.4. Biodistribution studies

The in vivo characteristics and cancer targeting of [^{131}I]Y-BP was investigated in BALB/c nude mice ($n = 5$) with subcutaneous HT1376 bladder cancers. B16F10 xenograft tumor models ($n = 5$)

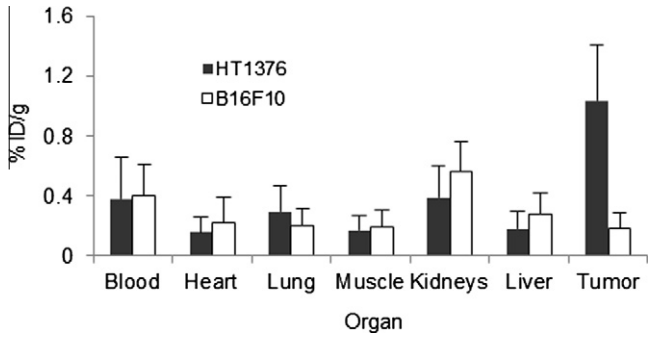

Figure 5. Biodistribution data of [^{131}I]Y-BP in mice bearing HT1376 human bladder cancer and B16F10 melanoma cells (n = 5). The mice were sacrificed at 5.5 h post-injection of [^{131}I]Y-BP.

were also used as a negative control. The organ distribution of [^{131}I]Y-BP at 5.5 h post-injection both in HT1376 and B16F10 xenograft tumor models was summarized in Figure 5. The 5.5 h post-injection, at which the highest tumor-to-background ratio was observed, was chosen as dissection time point based on a series of microPET images at different time points.

Radioactivity uptake for most non-specific organs was comparable or lower in HT1376 cancer bearing mice than in B16F10 tumor bearing mice. However, tumor uptake of [^{131}I]Y-BP in animals with HT1376 cancer cell almost six times higher in comparison to B16F10 tumor bearing mice. The tumor/blood, tumor/muscle, tumor/kidney and tumor/liver uptake ratios in HT1376 tumor bearing mice were found to be 2.7, 6.2, 2.7 and 5.9, respectively. This tumor targeting of the radiotracer was not observed in B16F10 tumor model at all, which clearly indicates that tumor accumulation of [^{131}I]Y-BP is a specific cell line targeting process. It was also observed that [^{131}I]Y-BP was cleared from the blood mainly via the renal pathway and to a lesser extent via the liver to the intestines.

The direct imaging of bladder cancer using [^{124}I]Y-BP seems to be hampered by high urine activity in bladder at early time point. However, the long half-life of ^{124}I (4.2 d) enables late imaging such as at 1 d post-injection. At 1 d post-injection of [^{124}I]Y-BP, the urine activity will be dropped dramatically and can be even lowered by using the diuretic agent. However, the better application of

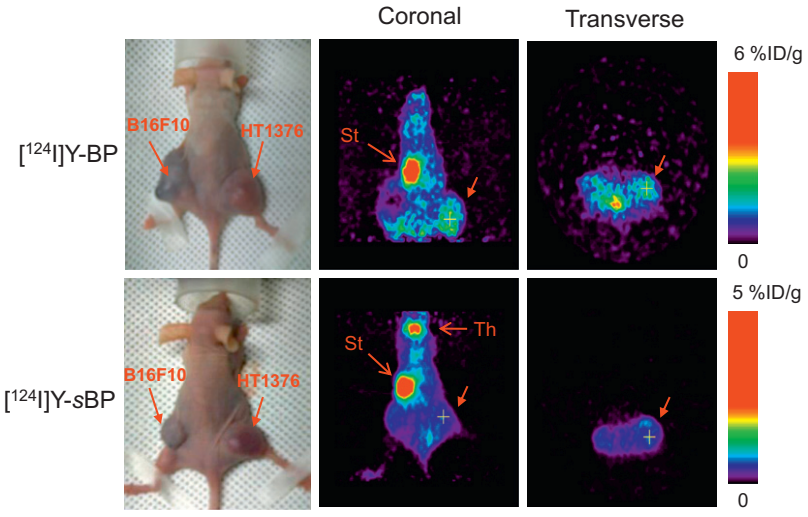

Figure 6. Typical microPET images of BALB/c nu/nu female mice bearing HT1376 bladder cancer and B16F10 melanoma on opposite flanks. Coronal (middle) and transverse images (right) at 5.5 h post-injection of [^{124}I]Y-BP and [^{124}I]Y-*s*BP are shown. The arrows indicate the HT1376 tumors. Th = thyroid, St = stomach.

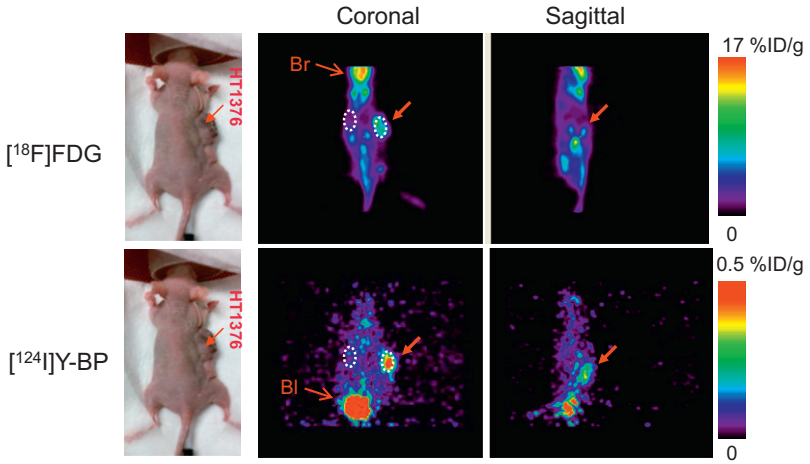

Figure 7. Comparative microPET images of [^{18}F]FDG and [^{124}I]Y-BP in the same xenograft mouse bearing HT1376 bladder cancer on the right flank. The transverse (right) and coronal (middle) images are shown. The microPET images were obtained at 40 min and 5.5 h after injection of 20 MBq of [^{18}F]FDG and 7.4 MBq of [^{124}I]Y-BP, respectively. The arrows indicate the HT1376 tumors. Br = brain, Bl = bladder. The white dotted circle shows the region selected for tumor-to-muscle ratio calculation.

[^{124}I]Y-BP will be found in the metastasized bladder cancer in other organs rather than primary bladder cancer.

3. Conclusion

In this study, the bladder cancer specific peptide, Y-BP with its scrambled version, Y-*s*BP, were radiolabeled with [^{131}I]NaI or [^{124}I]NaI and evaluated in xenograft bladder cancer models as a potential bladder cancer imaging agent. In consistent with the biodistribution result, [^{124}I]Y-BP showed highly selective uptake in HT1376 human bladder cancer models in microPET imaging studies. However, tumor targeting of [^{124}I]Y-BP was not observed when tested using B16F10 melanoma tumor model, indicating that tumor accumulation was a receptor-mediated specific process. Furthermore, [^{124}I]Y-BP showed superior tumor-to-background ratio in bladder cancer model compared to [^{18}F]FDG. All these experimental data suggest that [^{124}I]Y-BP can be considered as a potential radiopharmaceutical for the non-invasive diagnosis of bladder cancer, especially metastasized bladder cancer using PET.

4. Materials and methods

4.1. Peptides

Bladder cancer-specific peptides having the sequence, Cys-Ser-Asn-Arg-Asp-Ala-Arg-Arg-Cys (CSNRDARRC, all in L-isomer form), were synthesized by standard Fmoc methods and tyrosine residue was added to the N-terminal position before their cleavage from the resin. Then, the cleaved peptides were cyclized by disulfide bond formation between the two cysteine residues at the terminal positions (Y-BP). As a control, the seven amino acid sequences between the two cysteines were randomized to give scrambled peptides of the sequence, Cys-Asp-Ala-Ser-Arg-Arg-Asn-Arg-Cys which latter were also conjugated with tyrosine in the same way as above (Y-*s*BP). Both peptides were then purified and characterized by HPLC and LC-MS, respectively.

4.2. Radiolabeling study

[^{131}I]NaI in 0.1 M NaOH was purchased from Korea Atomic Energy Research Institute (Korea) and [^{124}I]NaI was kindly provided from the Korea Institute of Radiology and Science (KIRAMS, Seoul, Korea). The two peptides, Y-BP and Y-*s*BP, were labeled with [^{131}I]NaI or [^{124}I]NaI using Iodo-beads or Iodogen (Pierce Biochemical Co., Illinois, USA) to give the radioiodinated peptides, [$^{131/124}$I]Y-BP and [^{124}I]Y-*s*BP, respectively.[28] Briefly, in case of Iodo-beads method, a bead was washed in phosphate buffered saline (PBS, pH 7.2), dried on filter paper at room temperature and then was added to a solution of [$^{131/124}$I]NaI in 100 μL PBS. Following 5 min of shaking, peptide (20 μg in 20 μL of distilled water) was added to the solution and incubated at room temperature for 15 min under gentle shaking. The iodination was stopped by removing bead from the reaction tube. When Iodogen tube was used, 80 μL PBS was added to Iodogen tube and the necessary amount of [$^{131/124}$I]NaI was added. Then, the same amount of peptide (20 μg in 20 μL of distilled water) was added to the Iodogen tube and the mixture was allowed to stand for 15 min at room temperature after gentle shaking. The mixture was filtered through 0.22 μm syringe filter before HPLC injection.

The labeling yield was monitored by a radio-TLC imaging scanner (Bioscan, Inc., Washington, DC, USA) on a silica plate using 10% ammonium acetate:methanol (3:7) as the developing solvent. The labeled peptides were purified using an HPLC system (Waters 600, Milford, MA, USA), incorporating a reverse-phase GraceSmart RP C18 column (5 μm, 4.6 × 250 mm; Deerfield, IL, USA) at a flow rate of 1 mL/min, linear gradient from 97% solvent A (water with 0.1% trifluoroacetic acid) and 3% solvent B (acetonitrile with 0.1% trifluoroacetic acid) to 20% solvent A and 80% solvent B over a period of 30 min. The UV chromatogram was monitored using 220 nm wavelength. The collected fraction was concentrated under reduced pressure using rotary evaporator at maximum 40 °C bath setting, then diluted with saline for use in following in vitro and in vivo animal experiments.

4.3. Serum stability test

Stability of the radiolabeled peptide, [^{131}I]Y-BP in either Phosphate Buffered Saline (PBS) or Fetal Bovine Serum (FBS) was evaluated by incubation at 37 °C for 24 h. Briefly, radiolabeled [^{131}I]Y-BP (50 μL, 100 μCi) was incubated at 37 °C with gently shaking in either PBS or FBS (450 μL). The reaction aliquot were removed at 0, 1, 2, 3, 4, 5, 6 and 24 h post-incubation and the relative amount of intact parent radiolabled peptide was determined using radio-TLC over the study period. The same radio-TLC condition was used as above.

4.4. Animal models

All animal experiments were conducted in compliance with the Animal Care and Use Committee requirements of Kyungpook National University. Xenograft tumor models of human bladder cancer (HT1376) and melanoma (B16F10) cell lines for comparison study were prepared using 6 week-old BALB/c nu/nu female nude mice.[21] 5×10^6 HT1376 cells were inoculated subcutaneously into one side of flank of mice with or without B16F10 cells co-inoculated into the other flank of the mice. Tumors of appropriate size usually grew within 30 d (HT1376) and 12 d (B16F10) after the implantation of the respective tumor cells.

4.5. Biodistribution Studies

Biodistribution of [^{131}I]Y-BP was studied in BALB/c nu/nu female mice bearing HT1376 or B16F10 tumor. Mice were anesthetized with 1–2% isoflurane in O_2, and a volume of 0.1 mL of the purified [^{131}I]Y-BP solution (0.74 MBq) was then injected via a tail vein. Animals were sacrificed under anesthesia (isoflurane) at 5.5 h post-injection ($n = 5$). Blood, tumor, and tissues of interest were dissected, weighed, and counted in a γ-counter (Wallach, Turku, Finland). The percentage injected dose per gram (%ID/g) for each tissue was calculated.

4.6. MicroPET imaging

MicroPET images were acquired on a Concorde MicroPET R4 Rodent Model Scanner (Concorde Microsystems Inc., Knoxville, USA). Animals were anesthetized with isoflurane (1–2% in oxygen) and fixed in prone position on the bed.

MicroPET images of animals bearing HT1376 tumor and B16F10 on both flanks ($n = 3$) were acquired at 5.5 h post-injection of either radioiodinated [^{124}I]Y-BP or [^{124}I]Y-*s*BP (7.4 MBq in 0.15 mL saline) via tail vein.

For comparison study, tumor uptake of our radiotracer ([^{124}I]Y-BP) was compared with that of [^{18}F]FDG, the most widely used PET tracer for tumor detection. The microPET images of animals bearing HT1376 cancer cells ($n = 3$) were acquired for 20 min at 40 min post-injection of [^{18}F]FDG via tail vein (20 MBq). After 1 day, the same mice were injected again with 7.4 MBq of [^{124}I]Y-BP and scanned for 60 min at 5.5 h post-injection. Each 200 μL solution of $NaClO_4$ (20 mg/mL concentration) was injected orally and intraperitoneally 30 min earlier before [^{124}I]Y-BP injection to block free iodine uptake.[29] Another 200 μL solutions of Na-

ClO_4 solution was injected in the same way at 3 h post-injection of [^{124}I]Y-BP and microPET image was obtained at 5.5 h.

All microPET images were reconstructed by a 2-dimensional ordered-subsets expectation maximum (OSEM) algorithm and focal accumulations on microPET images were quantified by region of interest (ROI) analysis. Tumor-to-background ratios (T/B) were calculated using average counts per voxel on coronal images.

Acknowledgments

This work was supported by the Nuclear R&D (Grant code: 20090081817) and BAERI (Grant code: 20090078235) Programs of NRF, funded by MEST, and by the Korea Healthcare technology R&D Project, Ministry for Health, Welfare & Family Affairs (A102132). We thank Dr. Kyeong Min Kim for helpful discussion.

References and notes

1. Irani, J.; Mottet, N.; Caparros, M. J. R.; Teillac, P. *Eur. Urol., Suppl.* **2007**, *6*, 388.
2. Bassi, P.; De Marco, V.; De Lisa, A.; Mancini, M.; Pinto, F.; Bertoloni, R.; Longo, F. *Urol. Int.* **2005**, *75*, 193.
3. Papatsoris Athanasios, G.; Kachrilas, S.; Gekas, A. *Expert Opin. Investig. Drugs* **2007**, *16*, 1311.
4. Saad, A.; Hanbury, D. C.; McNicholas, T. A.; Boustead, G. B.; Morgan, S.; Woodman, A. C. *BJU Int.* **2002**, *89*, 369.
5. Jichlinski, P. *Curr. Opin. Urol.* **2003**, *13*, 351.
6. Saksena Mansi, A.; Dahl Douglas, M.; Harisinghani Mukesh, G. *World J. Urol.* **2006**, *24*, 473.
7. Raab, S. S.; Lenel, J. C.; Cohen, M. B. *Cancer* **1994**, *74*, 1621.
8. Bastacky, S.; Ibrahim, S.; Wilczynski, S. P.; Murphy, W. M. *Cancer* **1999**, *87*, 118.
9. Reske, S. N.; Kotzerke, J. *Eur. J. Nucl. Med.* **2001**, *28*, 1707.
10. Younes-Mhenni, S.; Janier, M. F.; Cinotti, L.; Antoine, J. C.; Tronc, F.; Cottin, V.; Ternamian, P. J.; Trouillas, P.; Honnorat, J. *Brain* **2004**, *127*, 2331.
11. Heicappell, R.; Muller-Mattheis, V.; Reinhardt, M.; Vosberg, H.; Gerharz, C. D.; Muller-Gartner, H.; Ackermann, R. *Eur. Urol.* **1999**, *36*, 582.
12. Bachor, R.; Kotzerke, J.; Reske, S. N.; Hautmann, R. *Urologe A* **1999**, *38*, 46.
13. Pinilla, I.; Rodriguez-Vigil, B.; Gomez-Leon, N. *Clin. Med.: Oncol.* **2008**, *2*, 181.
14. Dijkgraaf, I.; Boerman, O. C.; Oyen, W. J. G.; Corstens, F. H. M.; Gotthardt, M. *Anti-Cancer Agents Med. Chem.* **2007**, *7*, 543.
15. Okarvi, S. M. *Cancer Treat. Rev.* **2008**, *34*, 13.
16. Okarvi, S. M. *Med. Res. Rev.* **2004**, *24*, 357.
17. Schottelius, M.; Wester, H.-J. *Methods* **2009**, *48*, 161.
18. Reubi, J. C.; Maecke, H. R. *J. Nucl. Med.* **2008**, *49*, 1735.
19. Weiner, R. E.; Thakur, M. L. *Semin. Nucl. Med.* **2001**, *31*, 296.
20. de Jong, M.; Kwekkeboom, D.; Valkema, R.; Krenning, E. P. *Eur. J. Nucl. Med. Mol. Imaging* **2003**, *30*, 463.
21. Lee, S.-M.; Lee, E.-J.; Hong, H.-Y.; Kwon, M.-K.; Kwon, T.-H.; Choi, J.-Y.; Park, R.-W.; Kwon, T.-G.; Yoo, E.-S.; Yoon, G.-S.; Kim, I.-S.; Ruoslahti, E.; Lee, B.-H. *Mol. Cancer. Res.* **2007**, *5*, 11.
22. Samoylova, T. I.; Morrison, N. E.; Globa, L. P.; Cox, N. R. *Anti-Cancer Agents Med. Chem.* **2006**, *6*, 9.
23. Heppeler, A.; Froidevaux, S.; Eberle, A. N.; Maecke, H. R. *Curr. Med. Chem.* **2000**, *7*, 971.
24. Pentlow, K. S.; Graham, M. C.; Lambrecht, R. M.; Daghighian, F.; Bacharach, S. L.; Bendriem, B.; Finn, R. D.; Jordan, K.; Kalaigian, H., et al *J. Nucl. Med.* **1996**, *37*, 1557.
25. Bakker, W. H.; Krenning, E. P.; Breeman, W. A.; Koper, J. W.; Kooij, P. P.; Reubi, J. C.; Klijn, J. G.; Visser, T. J.; Docter, R.; Lamberts, S. W. *J. Nucl. Med.* **1990**, *31*, 1501.
26. Wolff, J. *Pharmacol. Rev.* **1998**, *50*, 89.
27. Huang, Y.-C.; Hsu, C.-C.; Huang, P.; Yin, T.-K.; Chiu, N.-T.; Wang, P.-W.; Huang, S.-H.; Huang, Y.-E. *NeuroImage* **2011**, *54*, 142.
28. Theibert, A. B.; Estevez, V. A.; Mourey, R. J.; Marecek, J. F.; Barrow, R. K.; Prestwich, G. D.; Snyder, S. H. *J. Biol. Chem.* **1992**, *267*, 9071.
29. Zuckier, L. S.; Li, Y.; Chang, C. J. *Cancer Biother Radiopharm* **1998**, *13*, 457.